JOURNAL OF CATALYSIS 9, 375–395 (1967)

The Kinetics of Propylene Disproportionation

J. W. BEGLEY* AND R. T. WILSON

From the Phillips Petroleum Company, Bartlesville, Oklahoma

Received August 2, 1967; revised October 16, 1967

Propylene disproportionation was studied using a tungsten-silica catalyst in an attempt to develop a kinetic model for design and optimization studies. The kinetics of the reaction were examined in terms of two mathematical models: (1) a model based upon the hypothesis of a second order reaction of adsorbed propylene molecules (Langmuir–Hinshelwood) and (2) a model developed for the hypothesized situation of a second order interaction of adsorbed molecules with molecules from the gas phase (Rideal). For those conditions where the catalyst surface conditions were thought to be equivalent, the Rideal model adequately correlated the data.

The results for the Rideal model suggest that the catalyst surface is saturated at high pressures (300–900 psia) and the rate of the reaction at a fixed temperature is controlled by the rate at which the reactive molecules strike the surface sites. The rate of reaction was examined in terms of a collision model.

The activation energy for the reaction was found to be 21.6 and 18.6 kcal/mole for two different catalysts. The variation of the activation energy with catalyst composition was found to be insignificant over the range of 3–12 wt % WO_3 on similar silica supports.

Propane in the propylene feed appeared to inhibit the reaction by adsorbing on the reaction sites. However, the ratio of the adsorption coefficients calculated by use of the data indicates that propane is more strongly adsorbed than propylene. This result is contrary to the firmly established knowledge of the relative adsorption characteristics and suggests that possibly a slight difference existed between the poisons level in the two feeds used in the study.

I. Introduction

The relatively recent discovery of highly selective catalysts for olefin disproportionation has led to considerable pilot plant and design studies of propylene disproportionation (*1*). In order to integrate this process with existing or projected facilities with optimum conditions, it is desirable to have a reliable kinetic expression for the main reaction as well as any important secondary reactions. Furthermore, kinetic studies aid in the determination of the reaction mechanism, which can be the basis for suggested improvements of the existing catalysts as well as add to the general knowledge of catalysis. It is also equally important that in doing a kinetic study the reaction is studied over a broad range of conditions, which gives valuable process information. The kinetic study is therefore a formal method of learning the characteristics of the reaction.

In the present study, pilot plant data from a small integral reactor were used to examine models of two possible mechanisms for propylene disproportionation. The mechanisms are interaction of two propylene molecules adsorbed on the catalyst surface (Langmuir–Hinshelwood) and interaction of an adsorbed molecule with a molecule from the gaseous or physically adsorbed states (Rideal).

II. Nomenclature

$C_2^=$	Ethylene concentration
$C_3^=$	Propylene concentration
C_3	Propane concentration
$C_4^=$	Butylene concentration
C_i	Concentration of impurities
$(C_3^=)_0$	Initial propylene concentration

* The Lummus Co., Bloomfield, New Jersey.

C_s	Concentration on the external catalyst particle surface
D_{eff}	Effective diffusion coefficient for a porous solid
$K_2^=$	Ethylene adsorption coefficient
$K_3^=$	Propylene adsorption coefficient
K_3	Propane adsorption coefficient
$K_4^=$	Butylene adsorption coefficient
K_i	Adsorption coefficient for impurities
K_{eq}	Equilibrium constant for the propylene disproportionation reaction
k_1	Forward reaction rate constant
k_2	Reverse reaction rate constant
n	Moles of reactant
R	Catalyst particle radius
t	Time
V	Volumetric rate of flow
V_c	Catalyst volume
X	Fraction of propylene unconverted
$\theta_2^=$	Fraction of sites covered by ethylene
$\theta_3^=$	Fraction of sites covered by propylene
θ_3	Fraction of sites covered by propane
$\theta_4^=$	Fraction of sites covered by butylenes
Φ	Dimensionless modulus

III. Experimental

Figure 1 shows a flow diagram of the pilot plant equipment. Feedstock contained in a cylinder was pressured by its own vapor pressure through a dryer and cooled in a coil immersed in either "wet" ice or dry ice to avoid vapor lock in the pump. The cooled liquid feed was pumped to the reactor by a Whitey laboratory diaphragm pump. The reactor was constructed from 1-inch Schedule 40 stainless steel pipe and fitted with an internal thermocouple well of 1/4-inch stainless steel tubing. The reactor temperature was maintained by five heaters, each on separate automatic control. The top of the reactor was filled with inert material and used as a feed vaporizer and preheater. The reactor pressure was maintained by a motor valve in the effluent line from the reactor. The low-pressure effluent gas passed through a glass trap, graduated in milliliters, to knock out any heavy liquid polymer which might be produced, thence through a wet test meter to a flare. The reactor effluent was analyzed by a chromatograph which was programmed and actuated by a TADS unit (Total Analysis Digital Systems—a unit designed and built by the Instrumentation and Automation Branch of Phillips Petroleum Company). Upon command the TADS unit would actuate the sampling of the gas stream by the chromatograph, then integrate, compute, normalize, and type out the analysis by means of an IBM electric typewriter. A complete analysis of the effluent gas stream

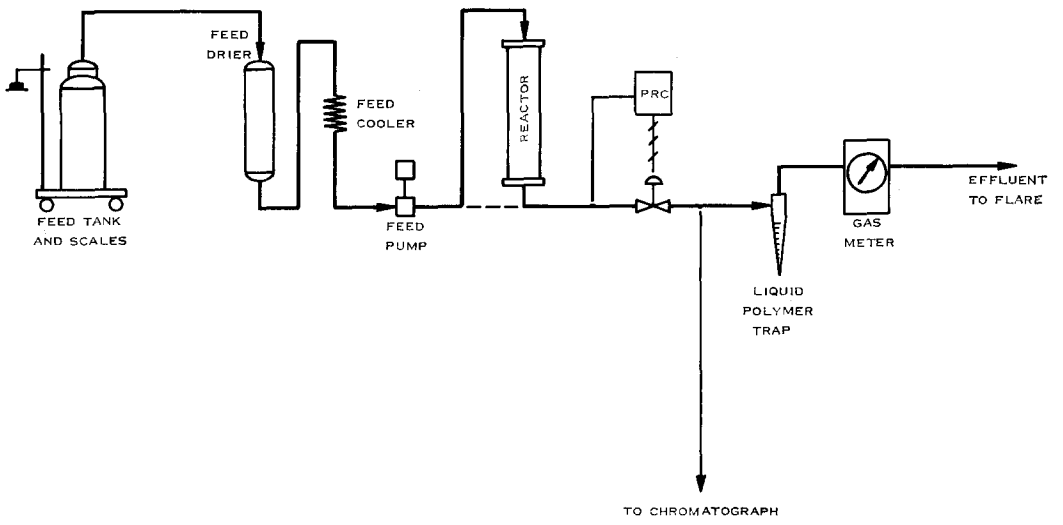

Fig. 1. Flow diagram of test apparatus; propylene disproportionation.

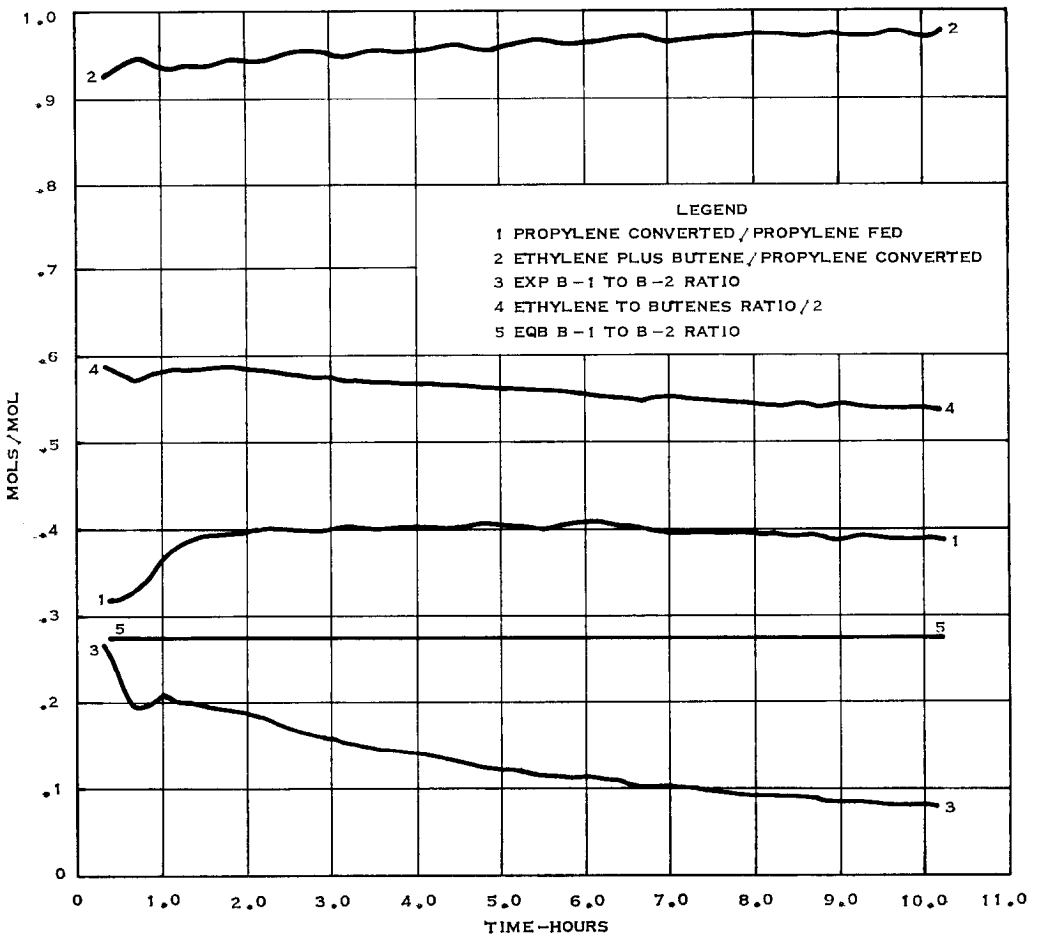

FIG. 2. Time plot of conversion, efficiency, etc.

and printout required approximately 10 min.

Regeneration of the catalyst was achieved by flushing the system with plant nitrogen followed by burning of the coke on the catalyst with a nitrogen and air mixture. An aliquot portion of the regeneration gas was collected over 20% sodium sulfate solution, and analyzed for CO and CO_2 by chromatograph to determine the carbon content of the catalyst.

The kinetic data are presented in Table 1. The feedstock used in most tests was either pure grade propylene or a blend containing 60 wt % propylene and 40 wt % propane, prepared from pure grade propylene and propane. The 60 wt % propylene content is typical of many plant propylene streams.

The same catalyst in the form of 1/8-inch extrudates containing 9 wt % WO_3 was used throughout most of the kinetic study. The reactor was flushed with nitrogen for approximately 15 min after the oxidation of the carbon on the catalyst. Figure 2 is a typical time plot of the conversion, efficiency, experimental and equilibrium butene-1–butene-2 ratios, and the ethylene–butene ratio. The conversion in all runs was taken to be an average of the values on the plateau. A computer program especially developed for this purpose was used to calculate and plot the data in Fig. 2 by use of chromatographic analyses of the feed and effluent streams as a function of time. The TADS unit was equipped to punch the chromatographic data on tape which was then fed to the IBM 7090 Computer.

TABLE 1
KINETIC DATA

Feed[a]	WHSV	Previous regeneration number	P (psig)	Temp. (°F)	Conv. (%)	Conv. averaged over Δt (hr)	Wt % C on catalyst	Efficiency (%)	B-1/B-2	Equil. B-1/B-2	Ethylene Butene
(1)	52.6	17	450	600°	4.35	0.3–2.4	—	99.91	0.095	0.198	1.166
				650°	6.87	3.0	—	99.91	0.113	0.217	1.126
				700°	14.10	1.7–3.0	—	97.15	0.124	0.236	1.058
				750°	27.33	2.0–2.3	—	96.84	0.131	0.255	1.089
				800°	38.56	3.0	—	95.74	0.117	0.274	1.102
				850°	43.98	2.7	7.3[b]	94.90	0.122	0.293	1.115
(1)	51.8	18	300	850°	42.14	5.9	7.5	94.91	0.125	0.293	1.135
(1)	54.5	19	600	800°	40.93	6.6	8.1	94.76	0.142	0.274	1.135
(1)	53.3	20	900	600°	7.19	0–7.2	—	95.13	0.139	0.198	1.161
				650°	12.17	0.4–2.4	—	96.51	0.146	0.217	1.114
				700°	21.90	2.0–3.0	—	96.78	0.139	0.236	1.107
				750°	35.34	1.0–2.0	—	95.50	0.136	0.255	1.123
				800°	42.89	0.3–1.8	5.5[b]	93.46	0.156	0.274	1.141
(1)	11.7	25	15	700°	1.56	6.2	—	100.00	0.075	0.236	1.456
				750°	8.03	2.2	—	96.48	0.074	0.255	1.138
				800°	35.16	3.2	2.6[b]	96.24	0.106	0.274	1.119
(1)	31.2	26	15	750°	8.99	3.4–3.8	—	97.88	0.40	0.255	1.128
				800°	20.36	3.2	—	96.95	0.052	0.274	1.096
				850°	31.91	3.0	2.7[b]	96.94	0.057	0.293	1.088
(2)	54.2	32	900	600°	7.21	3.0	—	98.98	0.066	0.188	1.036
				650°	19.13	4.2	1.8[b]	98.25	0.003	0.217	1.044
(2)	50.8	34	900	675°	31.80	7.7	—	97.75	0.059	0.227	1.050
				700°	38.27	5.8	5.0[b]	97.82	0.55	0.236	1.058
(1)	52.4	35	450	600°	10.58	3.5	—	99.1	0.076	0.198	1.099
				650°	11.14	1.8–3.6	—	99.43	0.098	0.217	1.122
				700°	19.10	3.1	—	97.74	0.101	0.236	1.104
				750°	30.08	2.7	—	96.59	0.115	0.255	1.124
				800°	40.06	3.0	—	95.45	0.109	0.274	1.130
				850°	43.78	1.8	6.2[b]	94.50	0.100	0.293	1.141
(1)	50.7	36	100	650°	4.23	3.6–6.0	—	97.71	0.070	0.217	1.229
				700°	7.43	1.0–4.3	—	98.62	0.070	0.236	1.134
				750°	14.06	2.3–2.8	—	98.55	0.069	0.255	1.113
				800°	26.80	3.9	—	97.72	0.062	0.274	1.094
				850°	36.74	3.0	4.3[b]	97.04	0.06	0.293	1.096
(2)	30	37	100	700°	21.9	10.0	5.3				
(2)	5.8	65	15	800°	41.50	8.2–10.8	1.3	97.09	0.082	0.2746	1.091
(2)	5.4	66	15	750°	31.10	10.1	1.2	98.01	0.077	0.255	1.070
(2)	4.9	67	40	750°	42.50	17.7–19.9	1.2	97.80	0.1157	0.255	1.108
(2)	10.2	68	15	800°	40.20	16.1–18.5	1.4	98.11	0.0466	0.274	1.062
(2)	10.1	69	40	750°	35.20	17.7–19.9	1.8	97.18	0.086	0.255	1.056
(2)	10.7	70	100	700°	37.00	18.2–19.9	1.2	97.66	0.0738	0.236	1.075
(2)	40.3	71	100	800°	38.80	3.3–9.6	1.5	98.04	0.45	0.274	1.064
(2)	41.1	73	240	750°	36.70	10.0	2.3	98.77	0.055	0.255	1.068
(2)	41.8	74	15	750°	18.57	5.4–6.8	—	100.00	0.023	0.255	1.012
			100	—	36.50	17.75	—	99.89	0.024	0.255	1.040
			450	—	43.0	5.5	—	98.05	0.063	0.255	1.090
			15	—	20.93	9.5	4.1[b]	98.74	0.012	0.255	1.034

TABLE 1 (*Continued*)

Feed[a]	WHSV	Previous regeneration number	P (psig)	Temp. (°F)	Conv. (%)	Conv. averaged over Δt (hr)	Wt % C on catalyst	Efficiency (%)	B-1/B-2	Equil. B-1/B-2	Ethylene Butene
(2)	41.0	75	450	700°	36.30	14.6	2.8	98.73	0.050	0.236	1.064
(2)	80.9	76	240	800°	35.2	14.8–16.7	6.3	99.68	0.0200	0.274	1.049
(1)	38.8	79	450	750°	30.0	12.7	5.0	97.62	0.096	0.255	1.096
(1)	33.7	80	450	800°	38.0	1.2–7.6	18.4	95.99	0.112	0.274	1.148
(1)	52.2	81	450	825°	44.0	8.3–12.2	52.2	95.79	0.082	0.283	1.0922
(2)	68.8	82	450	750°	34.3	1.9–6.83	4.2	98.69	0.0460	0.255	1.071
(2)	86.0	83	900	700°	29.6	3.9–6.0	1.9	98.78	0.056	0.236	1.082
(2)	82.3	84	450	750°	28.3	3.4–8.2	3.8	99.25	0.046	0.255	1.068
	74.1										
(2)	51.2	104	450	650°	10.9	8.3	2.5[b]	99.1	0.086	0.217	0.76
				700°	21.8	9.5	—	97.1	0.112	0.236	0.87
				750°	34.5	9.0	—	96.9	0.091	0.255	0.90

[a] (1) 65/35 propylene/propane; (2) 99 + propylene.

[b] Carbon determination after last data point for each run.

IV. Possible Controlling Mechanisms

There are several possible rate-controlling mechanisms in a catalytic system such as propylene disproportionation. Most of these at some time have been treated separately under ideal experimental conditions but unfortunately, have not been adequately considered in many catalyst systems in the past. The mechanisms are

(1) Diffusion of the reactant to the surface
(2) Adsorption on the surface
(3) Reaction on the surface
(4) Desorption of the products on the surface
(5) Diffusion of the products from the surface

Some of these mechanisms can be examined on a theoretical basis using the properties of the system to determine whether or not it is physically possible for them to be a controlling factor.

Using the methods outlined by Satterfield and Sherwood (*2*), the effectiveness factor for the catalyst extrudates was estimated to be near 1. On the basis of this result, diffusion of the reactant to the catalyst surface can be eliminated as a possible controlling factor. The calculation of the effectiveness factor is based upon the following characteristics for the 1/8-inch extrudates which were used to obtain the data in Table 1: pore volume, 0.8 cc/g; surface area, 314 m^2/g; and pore diameter, 114 Å.

The general criterion defining insignificant diffusion conditions (*2*) is, depending upon the order of the reaction,

$$\Phi = \frac{R^2}{D_{\text{eff}}}\left[-\frac{1}{V_c}\frac{dn}{dt}\right]\frac{1}{C_s} \leq 0.3 - 6.0$$

where R is the radius of the catalyst particle; D_{eff}, the effective diffusion coefficient for a porous solid; V_c, catalyst particle volume; dn/dt, reaction rate in the volume, V_c; and C_s, concentration at the surface of the particle. The value of Φ for the 1/8-inch extrudates containing 9% WO_3 was estimated using the data from the run at 29.7 psia and 750°F in Table 1 to determine a reaction rate. The value of Φ, 0.6, is lower than the value of 1.0 where diffusion begins to be significant for a first order reaction. It has been demonstrated that the rate of propylene disproportionation is pseudo first order. Consequently, diffusion does not appear to be significant for the extrudates.

The mass transfer rate from the bulk of the gas stream to the external catalyst particle surface is another possible rate-controlling step due to mass transfer. An estimate of this mass transfer rate was made and found to be large compared to the reaction rate. This result is consistent with

the rule of thumb that external diffusion cannot be a factor if the internal diffusion is not significant.

An estimate of the rate of adsorption on the surface of the catalyst can be made by considering the rate of collision of the gas molecules with the surface. The rate of impact can be calculated using the following equation from the kinetic theory of gases:

Rate of collision

$$= P/(2\pi mkT)^{1/2} \text{ molecules/cm}^2 \text{ sec}$$

At a pressure of 15 psig and 800°F, the rate of collision for pure propylene is 3.2×10^{23} molecules/cm^2 sec. The rate of adsorption will depend also upon the activation energy for adsorption, the surface coverage, and sticking coefficient. Therefore, the rate of adsorption becomes

Rate of adsorption

$$= [P/(2\pi mkT)^{1/2}]\alpha(1 - \theta) \exp(-E_s/RT)$$

where θ is the fraction of the sites covered by adsorbent; α, the probability of sticking; and E_s, the activation energy for adsorption. The most conservative estimate for the rate of adsorption is represented by the case of high surface coverage where $1 - \theta$ and α are small and E_s is large. With $1 - \theta = 0.1$, $\alpha = 10^{-4}$, and $E_s = 10$ kcal, the rate of adsorption is 2.24×10^{15} molecules/cm^2 sec. The value for α was taken from the curve for nitrogen adsorption on tungsten ribbon in the book by Ashmore (*3*). For the run at 29.7 psia and 750°F in Table 1, the rate of reaction is 2.36×10^{12} molecules/cm^2 sec. Therefore, the rate of adsorption is 1000 times the reaction rate for the case where rather low values for the surface coverage and sticking coefficient were used. On this basis, the rate of adsorption is considered to be fast compared to reaction.

The desorption of the products from the surface of the catalyst may be a significant factor in the rate of reaction but it is difficult to estimate this rate. If the adsorption isotherms for the products were known, an estimate could be made on the basis of the forward and backward rates being equal at equilibrium. However, adsorption isotherms are not available and are difficult to obtain because of the reaction which would occur during the attempt to obtain the isotherms.

Because of the unknown contributions of several factors to the overall reaction rate, it is somewhat of a trial-and-error process to arrive at a kinetic model based on certain hypotheses and some experimental data. In the present study, two different mechanisms were hypothesized and the kinetic model derived for each mechanism was tested using the data in Table 1. The derivations of the models are presented in the Appendix. The first one, represented by Eq. (11) of the Appendix, is based upon a second order surface reaction between two adsorbed propylene molecules with a reverse reaction between adsorbed butylene and ethylene molecules. This model is designated as the Langmuir–Hinshelwood model.

$$\tanh^{-1}\frac{2(K_{eq} - \tfrac{1}{4})X + \tfrac{1}{2}}{K_{eq}^{1/2}} - \tanh^{-1} \times \frac{2(K_{eq} - \tfrac{1}{4}) + \tfrac{1}{2}}{K_{eq}^{1/2}} = \frac{1}{V(C_3^=)_0} \times \frac{V_c k_2 K_{eq}^{1/2}}{\{[1 + K_3^=(C_3^=)_0 + \Sigma K_i C_i]/K_3^=(C_3^=)_0\}^2} \quad (11)$$

The second model is based upon an assumed second order reaction between adsorbed propylene molecules and molecules of propylene striking the surface from the gas phase. The kinetic model is very similar to Eq. (11) and is designated as the Rideal model [Appendix Eq. (18)].

$$\tanh^{-1}\frac{2(K_{eq} - \tfrac{1}{4})X + \tfrac{1}{2}}{K_{eq}^{1/2}} - \tanh^{-1} \times \frac{2(K_{eq} - \tfrac{1}{4}) + \tfrac{1}{2}}{K_{eq}^{1/2}} = \frac{V_c k_2 K_{eq}^{1/2}}{V\{[1 + K_3^=(C_3^=)_0 + \Sigma K_i C_i]/K_3^=(C_3^=)_0\}} \quad (18)$$

The only differences between Eqs. (11) and (18) are the initial concentration of propylene, $(C_3^=)_0$, in the denominator of the right side of Eq. (11) which does not appear in Eq. (18) and the square on the inhibition term in Eq. (11) which does not appear in Eq. (18). The left-hand sides of both equations are identical and can be evaluated when the percent conversion and tempera-

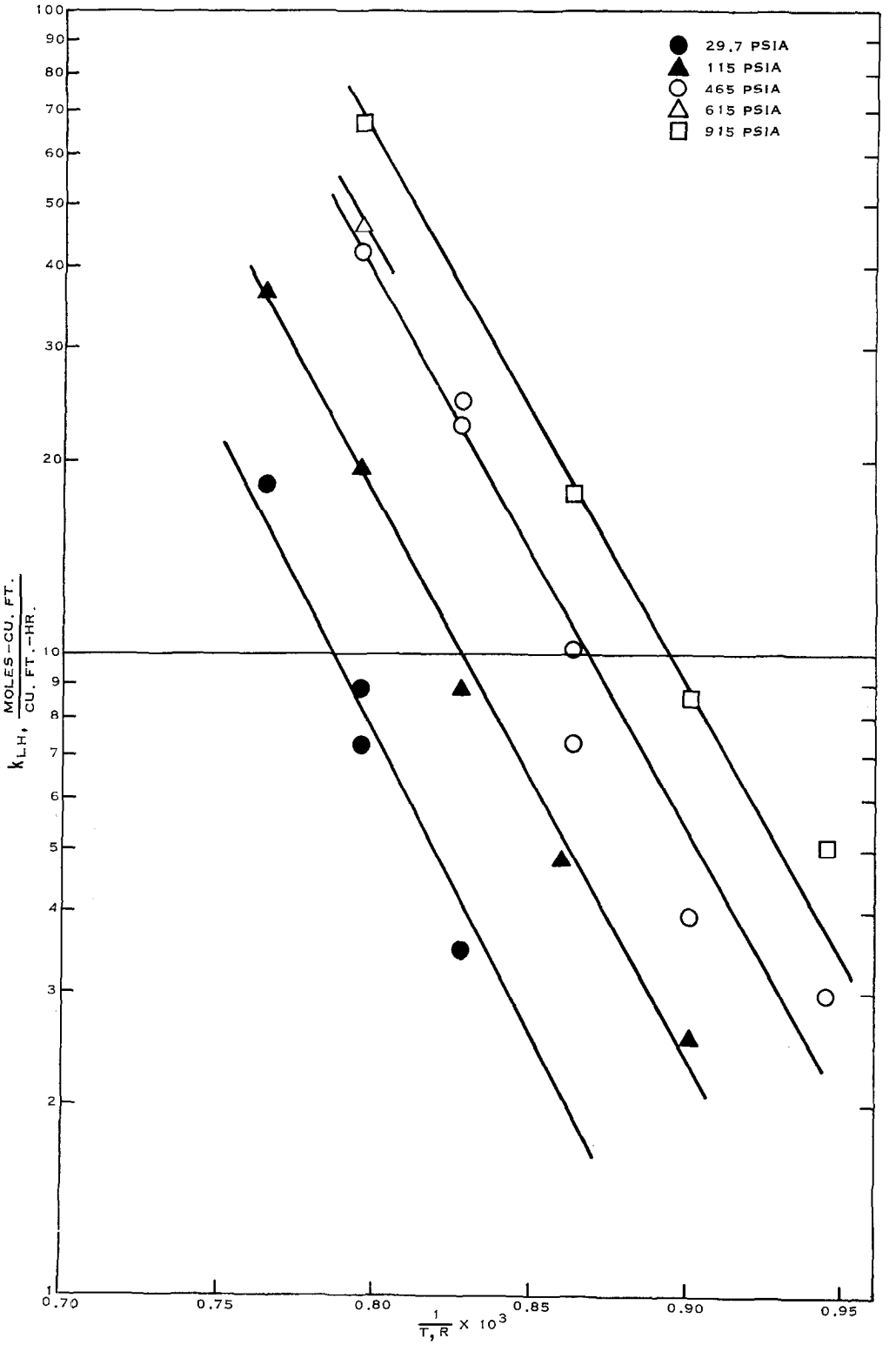

FIG. 3. Rate constants for Langmuir–Hinshelwood model.

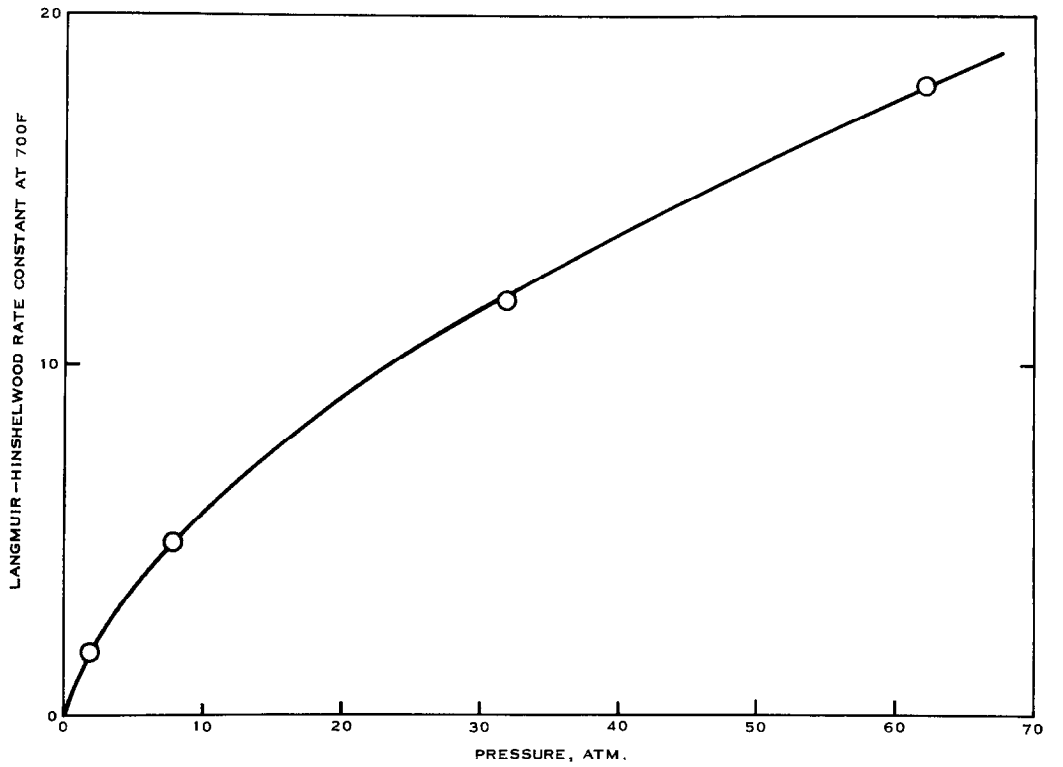

FIG. 4. Effect of pressure on Langmuir–Hinshelwood rate constant.

ture are known for a particular run. The rate constant which is complex can then be calculated using the value of the space velocity and the square root of the equilibrium constant. The equilibrium constant used in the present analysis is defined by $K_{eq} = K_t(1 + K_{ct})$, where K_t is the equilibrium constant for the reaction to *trans*-2-butene plus ethylene and K_{ct} is the equilibrium constant for the reaction between trans- and cis-2-butene. This assumes that the *cis*- and *trans*-butenes are in equilibrium.

V. Model Testing

The complex rate constants for the Langmuir–Hinshelwood model, i.e., are presented in Table 2 and Fig. 3. Only a portion of the data from Table 1 was used to prepare Table 2 and Fig. 3. The data should fit the functional form suggested by the complex

$$\frac{k_2}{\{[1 + K_3{=}(C_3{=})_0 + \Sigma K_i C_i]/K_3{=}(C_3{=})_0\}^2} = k_{LH}$$

rate constant, k_{LH}. However, a very simple test which can be used to show that the data do not fit this form consists of plotting the rate constant versus the initial propylene pressure. In Fig. 4, the data for 700°F are plotted in this fashion and the plot shows that the rate constant appears to increase without limit as pressure is increased. If the model were applicable the rate constant should approach a limiting value as pressure is increased and the surface sites become saturated with propylene. It is unlikely that the surface would not tend to saturate when the pressure is varied over the range indicated in Fig. 3 (~2–40 atm). The foregoing argument is therefore the basis for discounting the vailidity of the Langmuir–Hinshelwood model.

The rate constants for the Rideal model are presented in Table 3 and Figs. 5 and 6. The data at high pressures (300–900 psia) for each feed in Figs. 5 and 6 are represented by a common correlating line. The deviations are considerable in some cases, how-

TABLE 2
RATE CONSTANTS FOR LANMUIR–HINSHELWOOD MODEL

Feed[a]	P (psig)	V/V_c (ft³/ft³ hr)	Residence time[b] (sec)	Temp. (°F)	$(1/T,R) \times 10^3$	k_{LH} (moles ft³/ft³ hr)
(1)	450	850	1.70	600°	0.945	2.99
		898	1.60	650°	0.901	3.93
		969	1.49	700°	0.863	10.17
		986	1.46	750°	0.827	22.8
		1032	1.40	800°	0.795	42.25
(1)	600	803	1.79	800°	0.795	46.4
(1)	900	419	3.38	600°	0.945	5.08
		447	3.22	650°	0.901	8.55
		474	3.04	700°	0.863	17.9
				800°		67.0
(1)	15	3387	0.44	700°	0.863	0.216
		3540	0.41	750°	0.827	0.96
		3680	0.39	800°	0.795	7.2
(1)	15	9430	0.152	750°	0.827	3.48
		9800	0.148	800°	0.795	8.85
		10210	0.14	850°	0.765	18.42
(2)	900	434	3.32	600°	0.945	9.2
		465	3.10	650°	0.901	25.6
(2)	900	446	3.23	675°	0.882	43.9
(1)	450	841	1.71	600°	0.945	7.64
		872	1.62	650°	0.901	7.88
		933	1.54	700°	0.863	7.28
		986	1.46	750°	0.827	24.77
(1)	100	3600	0.40	650°	0.901	2.55
		3760	0.39	700°	0.860	4.81
		3943	0.36	750°	0.827	8.88
		4100	0.35	800°	0.795	19.56
		4270	0.33	850°	0.765	36.55

[a] (1) 65/35 propylene/propane; (2) 99 + propylene.
[b] Void fraction in reactor equals 0.4.

ever. The significant deviations are believed to be caused by differences in the catalyst surface conditions due to differences in conversion level or in the amount of adsorbed poisons on the catalyst which carry over from the regeneration and are not completely removed in the pretreatment period. Also, variations in the temperature setting may have contributed to these deviations. In addition, in those cases where the conversion approached the equilibrium conversion, small deviations in the percent conversion were magnified in the rate constant because of the nature of Eq. (18).

The Rideal model which is based upon the interaction of gas molecules with the adsorbed molecules appears to provide a basis for representing the data. For a fixed feed composition, the rate constants are essentially independent of pressure over a broad range (300–900 psia), which would indicate that the active-site coverage is independent of pressure over this range. In terms of the complex rate constant, this implies that the inhibition term becomes

$$1 + [K_i C_i / K_3{}^{=}(C_3{}^{=})_0]$$

and the rate constant is

$$\frac{k_2}{1 + [K_i C_i / K_3{}^{=}(C_3{}^{=})_0]}$$

TABLE 3
RATE CONSTANTS FOR RIDEAL MODEL

Feed[a]	P (psig)	V/V_c (ft³/ft³ hr)	Residence time[b] (sec)	Temp. (°F)	$(1/T,R) \times 10^3$	k_R (ft³/ft³ hr)
(1)	450	850	1.7	600°	0.945	113
		898	1.6	650°	0.901	155
		969	1.49	700°	0.863	420
		986	1.46	750°	0.827	982
		1032	1.40	800°	0.795	1894
(1)	600	803	1.79	800°	0.795	1570
(1)	900	419	3.38	600°	0.945	97.5
		447	3.22	650°	0.901	172
		474	3.04	700°	0.863	376
				800°	0.794	1527
(1)	15	3387	0.44	700°	0.863	140
		3540	0.41	750°	0.827	648
		3680	0.39	800°	0.795	5050
(1)	15	9430	0.152	750°	0.827	2350
		9800	0.148	800°	0.795	6200
		10210	0.14	850°	0.765	13460
(2)	900	434	3.32	600°	0.945	105
		465	3.10	650°	0.901	313
(2)	900	446	3.23	675°	0.882	586
(1)	450	892	1.62	650°	0.901	312
		933	1.54	700°	0.863	582
		986	1.46	750°	0.827	1067
(1)	100	3600	0.40	650°	0.901	407
		3760	0.39	700°	0.860	804
		3943	0.36	750°	0.827	1550
		4100	0.35	800°	0.795	3550
		4270	0.33	850°	0.765	6900
(2)	100	2260	0.64	700°	0.862	3360
(2)	15	1856	0.78	800°	0.795	4132
(2)	15	1660	0.87	750°	0.827	2006
(2)	15	3260	0.44	800°	0.795	7095
(2)	40	1680	0.86	750°	0.827	2680
(2)	100	809	1.78	700°	0.862	1390
(2)	100	3320	0.43	800°	0.795	6505
(2)	240	1453	0.99	750°	0.827	2667
(2)	15	12830	0.11	750°	0.827	7712
	100	3300	0.44	750°	0.827	5820
(2)	450	7450	0.19	700°	0.862	1350
(2)	240	2980	0.48	800°	0.795	4845
(1)	450	7300	0.20	750°	0.827	915
(1)	450	6610	0.22	800°	0.795	1180
(2)	450	1320	1.09	750°	0.827	2063
(2)	900	775	1.86	700°	0.862	966
(2)	450	1578	0.91	750°	0.827	1777
(2)	450	886	1.63	650°	0.801	306
		951	1.51	700°	0.863	739
		983	1.46	750°	0.826	1509

[a] (1) 65/35 propylene/propane; (2) 99 + propylene.
[b] Void fraction in the reactor equals 0.4.

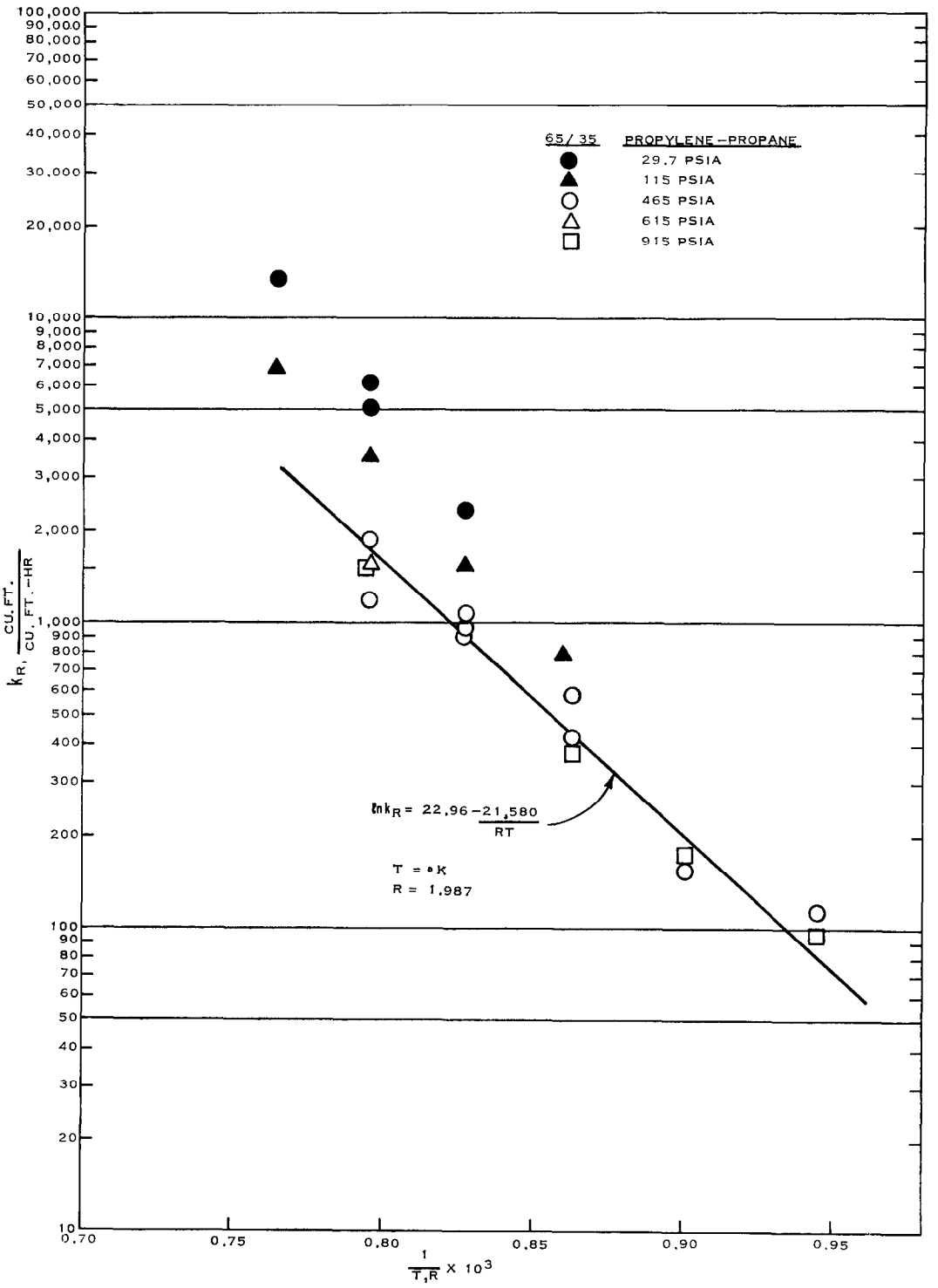

FIG. 5. Rate constants for Rideal mechanism.

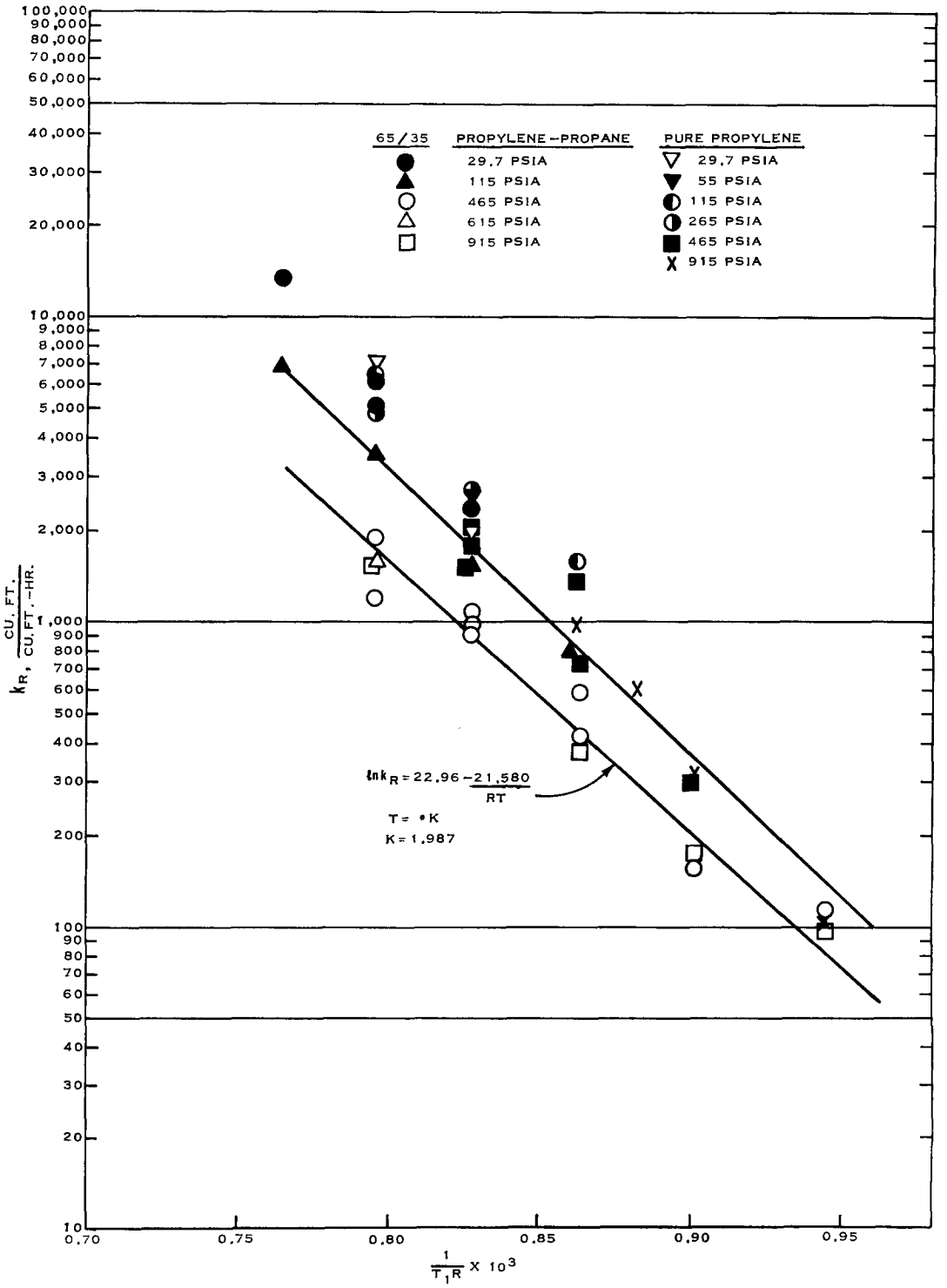

FIG. 6. Rate constants for Rideal mechanism.

TABLE 4
EFFECT OF PRETREATMENT ON CATALYST ACTIVITY AT LOW PRESSURES

WHSV	Psia	Hours on stream	Temp. (°F)	Conversion (%)	$(1/T.R) \times 10^3$	k_R (ft^3/ft^3 hr)
59.0	465	0–10	700°	38.5	0.861	2295
58.5	115	10–20	751°	35.6	0.825	6960
55.5	465	0–10	700°	37.7	0.861	1980
58.8	115	10–14	700°	23.6	0.861	3630
57.7	115	14–20	751°	31.7	0.826	6110
57.2	115	20–25	799°	38.9	0.795	9520

For a fixed feed composition, the term

$$1 + [K_i C_i / K_3{}^{=}(C_3{}^{=})_0]$$

is essentially constant and independent of temperature. Therefore, the temperature effect should correspond approximately to the activation energy of the gas–surface interaction.

The rate constants for the blend of propylene and propane at pressures near 115 and 29.7 psia are considerably higher than the constants at higher pressures. There are several possible factors which could individually or collectively contribute to this discrepancy. One of these factors is the pretreatment which is given the catalyst by the feed. The effect of the possible differences due to catalyst pretreatment was examined by making two different runs starting the reaction at 465 psia and lowering the pressure to 115 psia after steady state reaction conditions were established. The rate constants for the two conditions are compared in Table 4 and Fig. 7. The rate constants for the lower pressure are about two times as large as those at the higher pressure. This difference is comparable to that shown in Figs. 5 and 6, where the catalysts were conditioned at the run conditions. Therefore, catalyst pretreatment does not appear to be the problem.

Another possible explanation for the high rate constants at low pressures is a velocity effect. The runs at low pressure were made at a substantially higher linear velocity than for the runs at higher pressures. For example, the linear velocity at 15 psig was approximately 3.5–9.3 times as large as the velocity at 450 psig. Subsequent experiments with well-controlled conditions in a small laboratory reactor have been conducted; they indicate that the reaction on this catalyst is very definitely effected by the linear gas velocity. The results of this study will be reported at a later date.

The analysis of the two feeds used to obtain the rate data are presented in Table 5. One feed contained approximately

TABLE 5
CHROMATOGRAPHIC ANALYSES OF PROPYLENE FEEDS

	Propylene–propane blend (wt %)	Pure propylene (wt %)
Methane	0.03	0.05
Ethylene + Ethane	0.13	0.01
Propane	36.94	0.43
Propylene	62.42	99.06
n-Butane	0.15	0.05
1-Butene	0.08	0.08
trans-2-Butene	0.03	0.01
cis-2-Butene	0.03	0.00
Pentenes	0.19	0.31

65 mole % propylene and 35% propane. The other feed contained more than 99% propylene and was described as polymerization grade propylene. The rate constants for the case with the blend for feed are less than half the values for rate constants with pure propylene. If this difference is ascribed to the adsorption of propane on the surface sites, the adsorption constant for propane would have to be about twice the value for propylene. This result is contrary to established knowledge of the relative adsorption characteristics of propane and propylene and consequently does not appear to be a reasonable explanation. However, it can be

argued that the propane not only reduces the amount of adsorbed propylene on the surface but also acts to block the movement of propylene on the surface. A plausible explanation can be made on this basis. Of course, the apparent discrepancy can be very readily discounted as an effect of different poison levels in the two feeds. The tungsten catalyst is very susceptible to trace quantities of poisons such as water vapor, oxygen, hydrogen sulfide, acetylenes, and other compounds.

In Table 6 and Fig. 8, data are presented to show the effect of catalyst composition upon the Rideal rate constants. In the range of 6–12 wt % WO_3, the rate constants do not vary markedly but the values at 3 wt % are about half the values at the higher concentrations. The activation energies for the four tungstate catalysts are about the same value, 18.6 kcal/mole. This value is about 3 kcal/mole lower than for the catalyst used for the kinetic data reported in Table 1. The difference is attributed to catalyst age. The catalysts used to study the effects of catalyst composition were new catalysts which had not been regenerated more than one time. The data in Table 1 were obtained after the seventeenth regenerations.

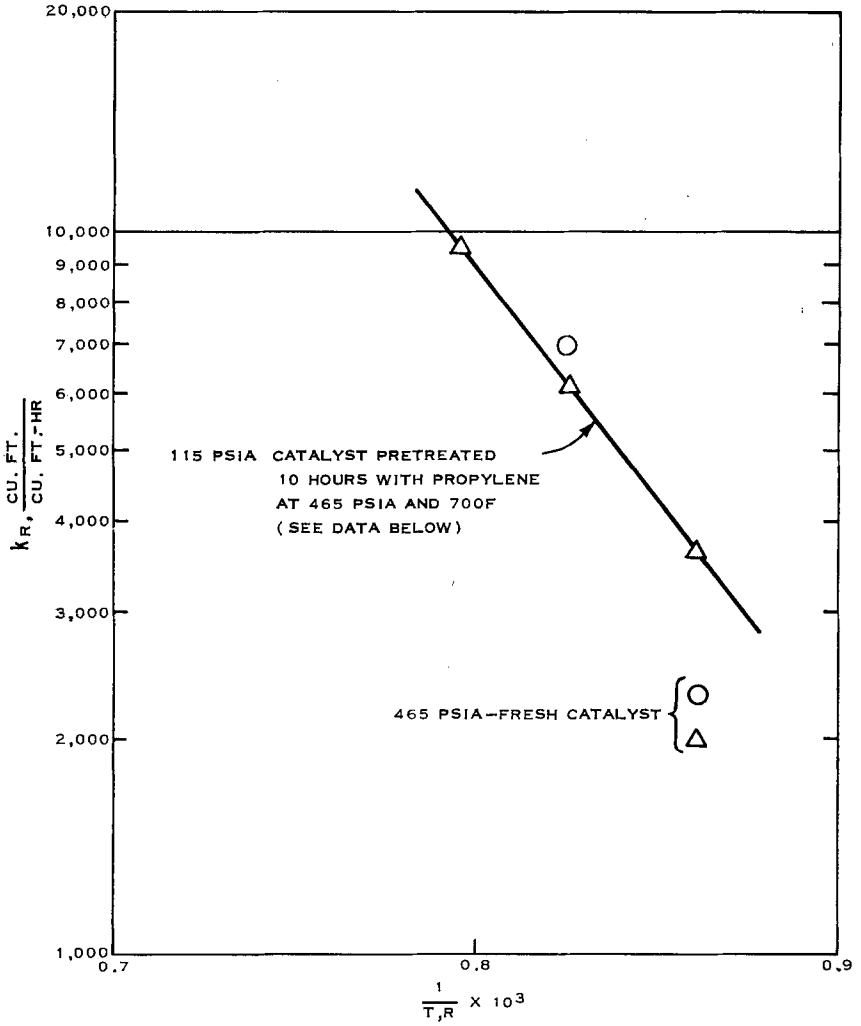

FIG. 7. Effect of pretreatment on catalyst activity at low pressures.

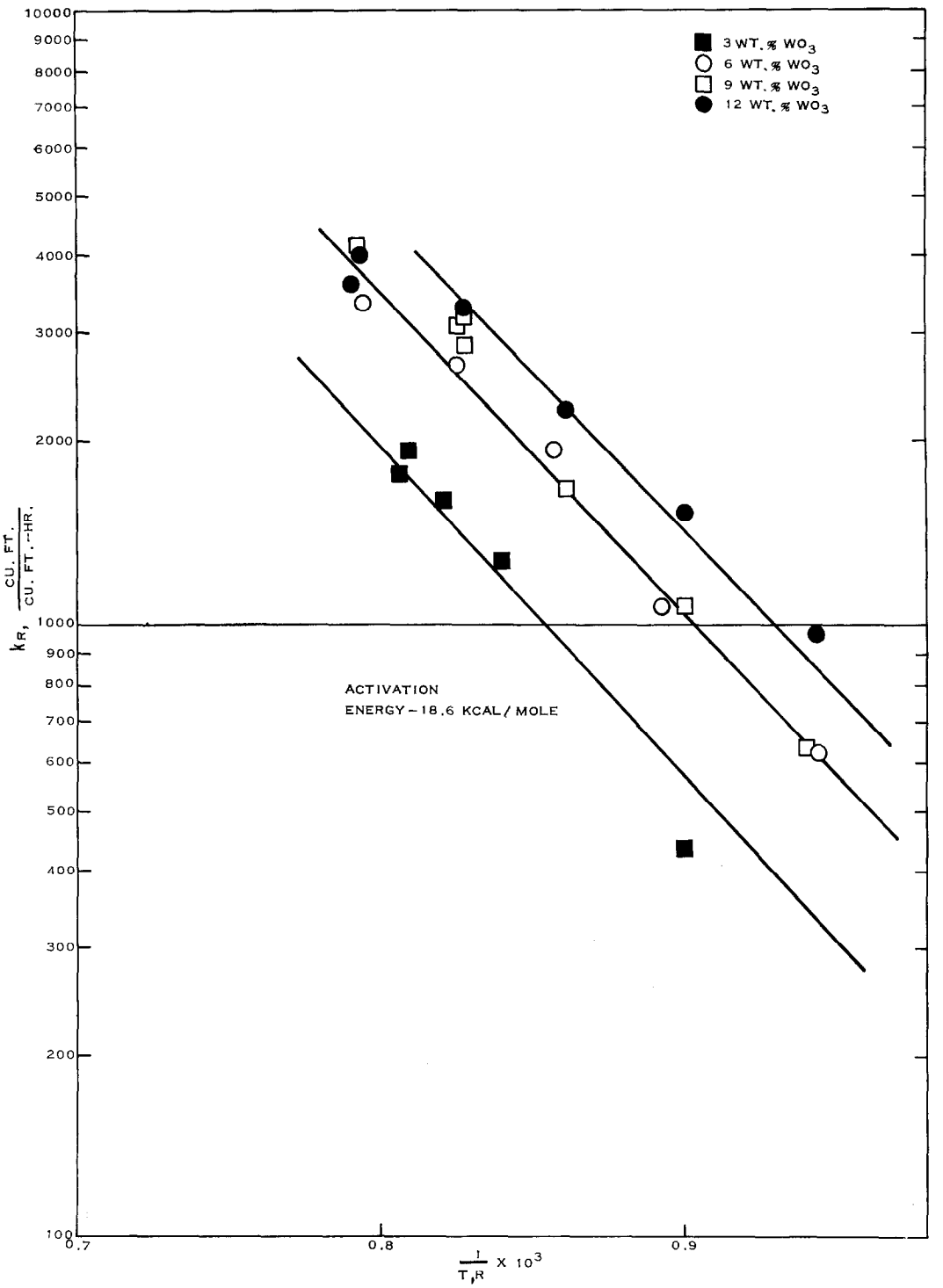

FIG. 8. Effect of catalyst composition on Rideal rate constants.

TABLE 6
EFFECT OF CATALYST COMPOSITION ON RIDEAL RATE CONSTANTS

Wt % WO_3	WHSV	Hours on stream (hr)	Temp. (°F)	Conversion (%)	$(1/T,R) \times 10^3$	k_R (ft^3/ft^3 hr)
3	63.2	0–10	780°	35.5	0.806	1757
		10–15	757°	34.1	0.821	1594
		20–25	651°	14.2	0.900	436
		25–30	775°	36.8	0.809	1910
6	67.3	0–9	799°	42.8	0.794	3345
		9–14	752°	40.1	0.825	2640
		14–20	707°	35.4	0.857	1923
		20–24	660°	26.7	0.893	1072
		24–29	600°	17.7	0.944	620
12	68.7	0–7	802°	44.4	0.792	4120
		7–11	750°	42.6	0.827	3165
		11–15	699°	30.5	0.864	1394
12	71.8	0–10	750°	40.5	0.827	2855
		10–14	700°	33.5	0.861	1669
		14–19	650°	25.8	0.900	1077
		19–24	606°	17.7	0.940	630
		24–29	751°	41.5	0.825	3053
9	59.4	0–10	802°	44.2	0.793	3360
		10–15	750°	42.4	0.827	3230
		15–20	701°	38.8	0.861	2247
		20–25	651°	32.5	0.900	1523
		25–30	600°	25.3	0.943	965
		30–34	804°	43.4	0.790	3582

VI. DISCUSSION OF KINETIC MODEL

The Rideal model has recently been proposed by Cvetanovic *et al.* as the mechanism for ethylene dimerization on alumina catalyst (*4*). For the ethylene reaction, a carbonium ion formation on Brönsted acid sites was suggested. The disproportionation reaction, however, probably occurs on sites which may be closer to Lewis acid sites.

It is of interest to examine the Rideal mechanism somewhat more in detail by comparing the known rate of reaction with the rate at which molecules strike the surface. The Rideal mechanism in the present case implies that the catalyst surface is saturated and the reaction rate is controlled by the rate of collision of the gas molecules with the surface. Where pure propylene at 650°F and 915 psia was used, the reaction rate is about 1.32×10^{13} molecules/cm^2 sec. The rate of the molecules striking the surface at these conditions is 10.3×10^{24}. If we use the experimental activation energy of 21.6 kcal/mole, the rate of reactive molecules (i.e., molecules containing the necessary reaction energy) striking the surface is 2.30×10^{17}. In other words, only one molecule in 17,500 which contains the necessary reaction energy reacts when it strikes the surface.

The surface is not completely covered with sites. For 9 wt % WO_3 on silica, the surface coverage by WO_3 is only 0.03. If the WO_3 is clustered and all sites are not covered with propylene, which must be the case for dynamic equilibrium, the fraction of surface covered by active sites may be near 0.01. Therefore, the ratio of the predicted reaction rate and the actual rate is about 175. This discrepancy can be attributed to a combination of factors which are (1) possible steric factor, (2) a slight error in the activation energy, and (3) an error in the number of surface sites. At 650°F a change of 2.8 kcal in the activation energy would be a factor of 10. The collision

model, therefore, predicts the following rate expression:

$$\text{Rate} = [P/(2\pi MRT)^{1/2}]\theta_3 = \exp(-E/RT) \quad \text{moles/cm}^2 \text{ sec}$$

where θ_3 is the fraction of total surface (not sites) covered by adsorbed propylene. This is identical to the Rideal model rate expression where the sites are saturated. Both models predict apparent first order kinetics. The accuracy of the prediction here is within the limits of expected accuracy for modern reaction rate theory. If the activation energy could have been predicted and the site concentration were known, the reaction rate could have been predicted a priori by use of the collision model.

The activation energies for the Rideal and Langmuir–Hinshelwood mechanisms would probably not be too different. If the reaction is controlled by the rate of molecules striking the surface as suggested by the results developed herein, there are two possible mechanisms to account for the interaction between the gas-phase and adsorbed-phase molecules. These are (1) the molecule striking the surface supplies the necessary energy to desorb the products, and (2) the molecule approaching the surface encounters an adsorbed propylene molecule and reacts, the energy of the molecule from the gas phase is used to desorb one of the products. In the former case the rate of desorption is rate-determining while in the latter, the surface reaction controls. The possibility of the rate of adsorption controlling is discounted on the basis of the Rideal rate constant being independent of pressure over the range of 300–900 psia.

The Langmuir–Hinshelwood and Rideal models were both derived using the assumption of perfect gas and ideal mixture behavior. Although the ideal mixture assumption is probably good over the range of conditions of interest in disproportionation, the assumption of perfect gas is not. This is particularly significant at low temperatures and high pressures, e.g., the conditions of temperature and pressure used with the cobalt-molybdena catalyst. At the higher temperature used with the tungsten-silica catalyst, the error in the rate constant judging from the value of compressibility factor cannot be greater than 10%. In order to eliminate possible deviations due to imperfect gas behavior, it is recommended that the right side of Eq. (18) be multiplied by the compressibility factor for propylene or the hydrocarbon mixture in use. The same compressibility factor should be used to calculate the volumetric flow rate. The rate constants in Table 3 and Figs. 5 and 6 were calculated on this basis.

VII. Analog Simulation of Propylene Disproportionation

The model represented by Eq. (18) plus the data in Figs. 5 and 6 can be used to predict propylene conversion for a given space rate, pressure, and temperature. In order to predict efficiency in possible process simulation and design studies, the relative rates of the secondary reactions are needed also. With the exception of a few minor reactions, the complete system of reversible reactions is outlined as follows:

$$2C_3H_6 \rightleftarrows C_4H_8\text{-}2 + C_2H_4 \quad \text{(a)}$$
$$C_4H_8\text{-}2 \rightleftarrows C_4H_8\text{-}1 \quad \text{(b)}$$
$$C_4H_8\text{-}1 + C_3H_6 \rightleftarrows C_5H_{10}\text{-}2 + C_2H_4 \quad \text{(c)}$$
$$C_4H_8\text{-}1 + C_4H_8\text{-}2 \rightleftarrows C_5H_{10}\text{-}2 + C_3H_6 \quad \text{(d)}$$
$$C_5H_{10}\text{-}2 \rightleftarrows C_5H_{10}\text{-}1 \quad \text{(e)}$$
$$C_5H_{10}\text{-}1 + C_3H_6 \rightleftarrows C_6H_{12}\text{-}2 \quad \text{(f)}$$
$$C_6H_{12}\text{-}2 \rightleftarrows C_6H_{12}\text{-}3 \quad \text{(g)}$$
$$C_6H_{12}\text{-}3 + C_2H_4 \rightleftarrows 2C_4H_8\text{-}1 \quad \text{(h)}$$
$$C_6H_{12}\text{-}2 + C_2H_4 \rightleftarrows C_5H_{10}\text{-}1 + C_3H_6 \quad \text{(i)}$$

The isomerization of *cis*- and *trans*-2-butene to 1-butene (b) appears to be the major reason for the propylene disproportionation reaction being less than essentially 100% efficient. On some catalysts ethylene dimerization to 1-butene can be significant. However, it is not important for the catalyst used in this study. The isomerization reaction is evident in the time plot in Fig. 2 where the efficiency gradually increases as the isomerization activity (1-butene/2-butene ratio) decreases during the run. The isomerization activity appears to be independent of the disproportionation activity, which indicates that the active sites are different for the two reactions. In order to solve the foregoing system of equations to predict the efficiency for any

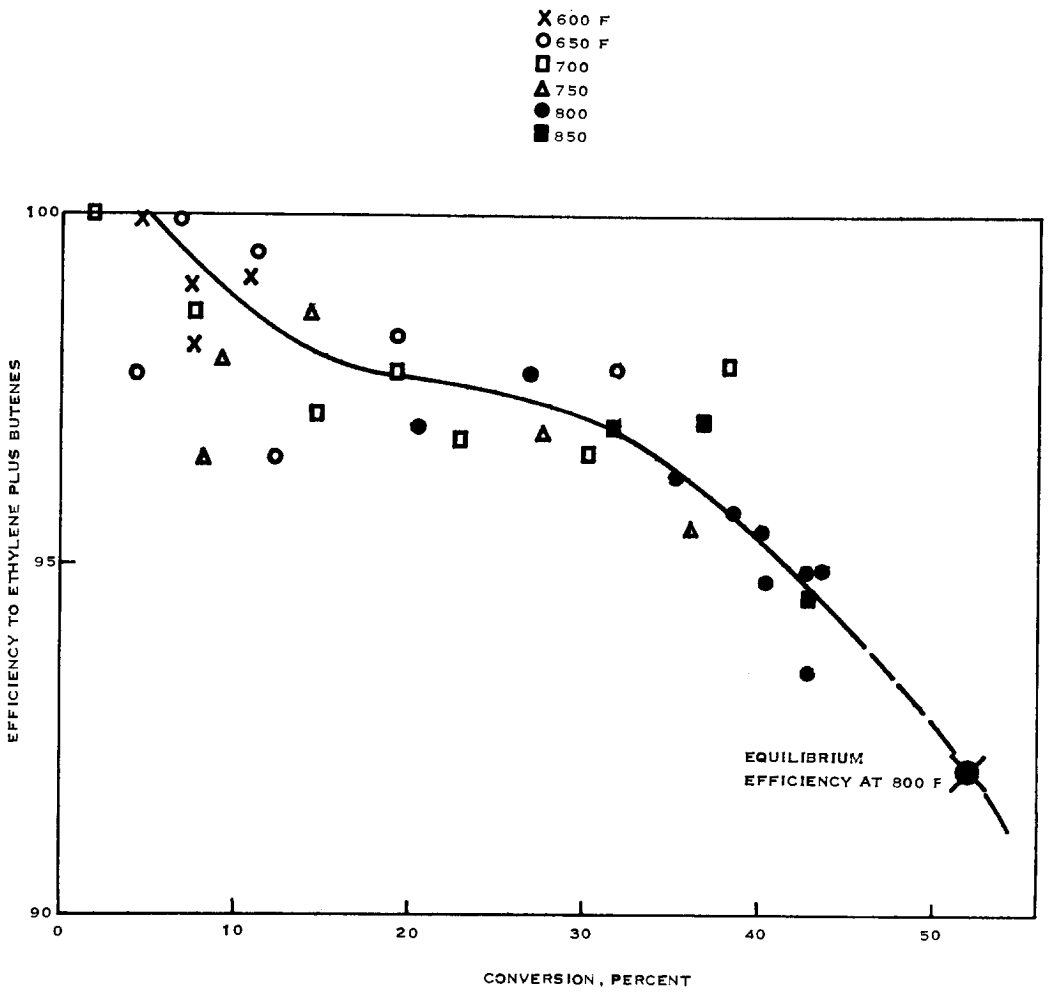

FIG. 9. Efficiency of propylene disproportionation to ethylene plus butenes.

specified product at least nine rate constants are required if the principle of microscopic reversibility is used to define the reverse rate constant by use of the equilibrium constants.

The analog computer has been used to examine the system of equations. The only meaningful results are the equilibrium distributions and efficiencies at two different temperatures, 800° and 980°F. The results are presented in Table 7. In Fig. 9, the efficiency for the runs reported in Table 1 are plotted versus percent conversion. The efficiency in this case is defined as the weight of ethylene plus butylene yield divided by the weight of propylene reacted. The temperature and pressure effects upon efficiency do not appear to be significant. The equilibrium conversion indicated in Fig. 9 is about eight percentage points higher than the highest experimental values which would seem to indicate that equilibrium conditions were not fully attained in any of the pilot plant runs.

VIII. Conclusions

(1) Propylene disproportionation kinetics were examined in terms of two mathematical models: Langmuir–Hinshelwood, which hypothesizes the interaction of two adsorbed propylene molecules, and Rideal, which is based on the hypothesis of the interaction of an absorbed molecule and a gas-phase molecule. The Rideal model was found to fit the data adequately when equivalent

TABLE 7
EQUILIBRIUM DISTRIBUTION (MOLE %) OF PRODUCTS FOR PROPYLENE DISPROPORTIONATION

	800°F	980°F
Ethylene	27.73	29.05
Propylene	47.40	46.25
1-Butene	4.47	5.41
2-Butene	17.99	15.85
Pentenes	2.18	2.61
Hexenes	0.30	0.86
Conversion	52.60	53.75
Wt % efficiency (ethylene + butenes)	92.08	88.77
Ethylene–butene ratio	1.23	1.37

surface conditions existed, i.e., at pressures 300–900 psia. The rate constants at lower pressures 30 and 115 psia were higher, possibly because of a change in the linear gas velocity in the catalyst bed.

(2) The activation energy for the reaction on an aged catalyst was determined to be 21.6 kcal/mole. On a new catalyst which had not been regenerated more than one time, the activation energy was 18.6 kcal/mole. The variation of activation energy with catalyst composition was insignificant over the range of 3–12 wt % WO_3.

(3) Although propane in the feed appeared to inhibit the reaction, the ratio of propane–propylene adsorption coefficients calculated by use of the data was unrealistic, indicating a possible poison in the propane–propylene feed.

APPENDIX

DERIVATION OF THE KINETIC MODEL

A. Langmuir–Hinshelwood Model

The fraction of surface sites which are covered by any one species in the system can be determined by use of the simple Langmuir-type adsorption, e.g., the fraction of surface sites covered by propylene is

$$\theta_3^{=} = \frac{K_3^{=}(C_3^{=})}{1 + K_3^{=}(C_3^{=}) + K_2^{=}(C_2^{=}) + K_4^{=}(C_4^{=}) + \Sigma K_i C_i} \quad (1)$$

If we assume that the forward reaction is controlled by the second order reaction of two adsorbed propylene molecules, then

$$-[d(C_3^{=})/dt]_f = 2k_1(\theta_3^{=})^2 \quad (2)$$

The reverse reaction is probably controlled principally by the second order reaction of adsorbed molecules of ethylene and butylenes. The disproportionation of the butylenes is slow as evidenced by the small yield of pentenes. Therefore, the net rate is

$$-\tfrac{1}{2}d(C_3^{=})/dt = k_1(\theta_3^{=})^2 - k_2(\theta_2^{=})(\theta_4^{=}) \quad (3)$$

If we use catalyst volume and volumetric feed rate to define time and substitute the respective equations similar to Eq. (1) into Eq. (3), the rate expression becomes

$$\frac{-\tfrac{1}{2}d(C_3^{=})}{dV_c} = \frac{k_1(K_3^{=})^2(C_3^{=})^2 - k_2K_2^{=}K_4^{=}(C_2^{=})(C_4^{=})}{[1 + K_3^{=}(C_3^{=}) + K_2^{=}(C_2^{=}) + K_4^{=}(C_4^{=}) + \Sigma K_iC_i]^2} \quad (4)$$

The inhibiting effect of the heavier olefins, pentenes, etc., is neglected in Eq. (4). The efficiency for the propylene disproportionation is greater than 95% in most cases and consequently, the effect of the heavier components should be small. The reverse reaction will not be completely described by the ethylene–butylene reaction but here again, the error is small. Because most of the disproportionation studies have been made using feeds containing certain impurities, the inhibiting effects of these components are indicated by ΣK_iC_i in Eq. (4).

Equation (4) contains several unknown factors and in order to determine every constant would probably require a prohibitive number of experiments. It is therefore necessary to make certain simplifying assumptions. Because of the relationship between the adsorption coefficients for ethylene, propylene, and butylene, it is probably a good assumption that (1) $K_2^{=}K_4^{=} = (K_3^{=})^2$ and (2) $K_3^{=}(C_3^{=}) + K_2^{=}(C_2^{=}) + K_4^{=}(C_4^{=}) = K_3^{=}(C_3^{=})_0$, where $(C_3^{=})_0$ is the initial propylene concentration. Assumptions (1) and (2) are equivalent to assuming that

the adsorption coefficients for the olefins are equal. However, because of the probable increase in the adsorption coefficient with increasing molecular weight, the assumptions could also be good in spite of the fact that the adsorption coefficients are not equal. Equation (4) is simplified considerably by the use of assumptions (1) and (2).

$$\frac{-\frac{1}{2}V\,d(C_3^=)}{dV_c} = \frac{(K_3^=)^2[k_1(C_3^=)^2 - k_2(C_2^=)(C_4^=)]}{[1 + K_3^=(C_3^=)_0 + K_iC_i]^2} \quad (5)$$

In order to transform Eq. (5) to an integrable form, the following definitions were used:

$$\frac{(C_3^=)}{(C_3^=)_0} = X \quad (6)$$

$$\frac{(C_3^=)_0 - (C_3^=)}{2(C_3^=)_0} = \frac{(C_2^=)}{(C_3^=)_0} = \frac{1 - X}{2} \quad (7)$$

$$\frac{(C_3^=)_0 - (C_3^=)}{2(C_3^=)_0} = \frac{(C_4^=)}{(C_3^=)_0} = \frac{1 - X}{2} \quad (8)$$

Equations (7) and (8) are valid for the case of 100% efficiency with a theoretical distribution of ethylene and butylenes. Because of the small amount of butylene disproportionation and possibly ethylene dimerization, the final kinetic expression will be only approximate but should be adequate for representing the data. The use of Eqs. (6), (7), and (8) in Eq. (5) leads to a form which can be integrated

$$\frac{-\frac{1}{2}V\,dX}{dV_c} = \frac{k_1X^2 - \frac{1}{4}k_2(1 - X)^2}{\{[1 + K_3^=(C_3^=)_0 + \Sigma K_iC_i]/K_3^=(C_3^=)_0\}^2} \quad (9)$$

$$\int_1^X \frac{dX}{(k_1 - \frac{1}{4}k_2)X^2 + \frac{1}{2}k_2X - \frac{1}{4}k_2} = -\int_0^{V_c} \times \frac{dV_c}{V(C_3^=)_0\{[1 + K_3^=(C_3^=)_0 + K_iC_i]/K_3^=(C_3^=)_0\}^2} \quad (10)$$

The left-hand side of Eq. (10) is of the form

$$\int \frac{dX}{\bar{X}} = \frac{-2}{-q^{1/2}} \tanh^{-1} \frac{2\,cX + b}{-q^{1/2}}$$

where $\bar{X} = a + bX + cX^2$

$$q = 4\,ac - b^2$$

Therefore in terms of the coefficients in Eq. (10)

$$a = \tfrac{1}{4} - k_2$$

$$b = \tfrac{1}{2}k_2$$

$$c = k_1 - \tfrac{1}{4}k_2$$

$$q = -k_1k_2$$

The rate constants for the forward and reverse reactions are related by the equilibrium constant, $K_{eq} = k_1/k_2$. The final integrated rate expression is

$$\tanh^{-1} \frac{2(K_{eq} - \frac{1}{4})X + \frac{1}{2}}{K_{eq}^{1/2}} - \tanh^{-1} \frac{2(K_{eq} - \frac{1}{4}) + \frac{1}{2}}{K_{eq}^{1/2}} = \frac{V_ck_2K_{eq}^{1/2}}{V(C_3^=)_0\{[1 + K_3^=(C_3^=)_0 + \Sigma K_iC_i]/K_3^=(C_3^=)_0\}^2} \quad (11)$$

B. Rideal Model

The Rideal model is based upon the assumed interaction of an adsorbed species and a species from the gas phase striking the surface or a species in a state of physical adsorption. For propylene disproportionation, the forward rate expression is

$$-[d(C_3^=)/dt_f = 2k_1\theta_3^=C_3^= \quad (12)$$

The reverse reaction rate expression contains two terms to account for the two distinct ways of interaction, i.e., an interaction between an adsorbed ethylene molecule and a butylene molecule from the gas phase plus the interaction of an adsorbed butylene molecule and an ethylene molecule from the gas phase

$$[d(C_3^=)/dt]_b = 2[k'\theta_2^=C_4^= + k''C_2^=\theta_4^=] \quad (13)$$

The net rate of disappearance of propylene is

$$-\tfrac{1}{2}d(C_3^=)/dt = k_1\theta_3^=C_3^= - k'\theta_2^=C_4^= - k''C_2^=\theta_4^= \quad (14)$$

By use of Eq. (1) and the definition for time, V_c/V, in addition to assuming that

$k' = k'' = k_2$, an expression similar to Eq. (4) is obtained.

$$\frac{-\frac{1}{2}Vd(C_3^=)}{dV_c} = \frac{k_1K_3^=(C_3^=)^2}{-k_2C_2^=C_4^=(K_2^= + K_4^=)} \Big/ [1 + K_2^=C_2^= + K_3^=C_3^= + K_4^=C_4^= + \Sigma K_iC_i] \quad (15)$$

If the term $(K_2^= + K_4^=)$ is approximated by $2K_3^=$, Eq. (15) becomes

$$\frac{-\frac{1}{2}Vd(C_3^=)}{dV_c} = \frac{k_1K_3^=(C_3^=)^2 - 2k_2K_3^=C_2^=C_4^=}{[1 + K_2^=C_2^= + K_3^=C_3^= + K_4^=C_4^= + \Sigma K_iC_i]} \quad (16)$$

Equation (16) can be integrated after substitution of Eqs. 6, 7, and 8 which define the concentrations in terms of unreacted propylene

$$\frac{-\frac{1}{2}VdX}{dV_c} = \frac{k_1X^2 - 2k_2\frac{1}{4}(1 - X)^2}{\{[1 + K_3^=(C_3^=)_0 + \Sigma K_iC_i]/K_3^=(C_3^=)_0\}} \quad (17)$$

Equation (17) is of the same form as Eq. (9) and can be integrated to give the following expression which is very similar to Eq. (11) except for the lack of the square on the inhibition factor

$$\{[1 + K_3^=(C_3^=)_0 + K_iC_i]/K_3^=(C_3^=)_0\}$$

and the initial propylene concentration in the denominator of the right-hand side.

$$\tanh^{-1}\frac{2(K_{eq} - \frac{1}{4})X + \frac{1}{2}}{K_{eq}^{1/2}} - \tanh^{-1}\frac{2(K_{eq} - \frac{1}{4}) + \frac{1}{2}}{K_{eq}^{1/2}} = \frac{V_ck_2K_{eq}^{1/2}}{V\{[1 + K_3^=(C_3^=)_0 + \Sigma K_iC_i]/K_3^=(C_3^=)_0\}} \quad (18)$$

References

1. Banks, R. L., and Bailey, G. C., *Ind. Eng. Chem.* **3**, 170 (1964).
2. Satterfield, C. N., and Sherwood, T. K., "The Role of Diffusion in Catalysis," p. 91. Addison-Wesley Publishing Co., Reading, Massachusetts, 1963.
3. Ashmore, P. G., "Catalysis and Inhibition of Chemical Reactions," p. 161. Butterworth, London, 1963.
4. Amenomiya, U., Chenier, J. H. B., and Cvetanovic, R. J., "Mechanism of Ethylene Polymerization on Alumina," presented at the Third International Congress on Catalysis, Amsterdam, 1964.